A MOLECULAR DYNAMICS INVESTIGATION ON FUEL VAPORIZATION AND MIXING CHARACTERISTICS UNDER SUB/SUPERCRITICAL CONDITIONS

by

Wu WEI[a], Tingyu ZHOU[a], Lun ZHAO[b,c*], Lei DENG[d], and Maozhao XIE[d]

[a] School of Mechanical Engineering, Guizhou University, Guiyang, China
[b] Institute of Intelligent Manufacturing Technology, Shenzhen Polytechnic, Shenzhen, China
[c] Shenzhen Institutes of Advanced Technology, Chinese Academy of Sciences, Shenzhen, China
[d] School of Energy and Power Engineering, Dalian University of Technology, Dalian, China

Original scientific paper
https://doi.org/10.2298/TSCI210201335W

Molecular dynamics simulation is performed to study the influence of environmental pressure on the mixing process. Based on the OPLS-AA full-atomic potential function, the gas-liquid-gas simulation box model is used to study the evaporation characteristics of n-heptane at different environmental conditions. The results show that compared with the subcritical environment, the nitrogen molecules in the supercritical condition can diffuse into the liquid phase region earlier, and the temperature of the liquid phase rise faster, and then a unified supercritical fluid could be formed. Based on the density profile, a gas-liquid-gas interface thickness is defined and the interface thickness is widened as the ambient pressure increase, resulting in the conventional subcritical evaporation transition turbulent mixing process.

Key words: *molecular dynamics simulation, pressure effect, mixing layer, vaporization and mixing characteristics*

Introduction

Nowadays, with the issue of energy security and environmental pollution becoming a hot topic, more and more researchers are working hard to develop high efficiency and low emission machines. Supercritical injection helps improve fuel combustion efficiency and reduce pollutant emissions, hence received widespread concern. Power machines such as hydrogen-oxygen rocket engine and internal combustion engine generally operate at conditions above the injected fuel critical point, where the mixing and vaporization processes are different from subcritical conditions [1, 2]. Under subcritical conditions, the injected fuel disintegrations are dominated by the action of surface tension, where ligament formation, atomization and droplet evaporation phenomenon usually take place. However, once the ambient pressure reach supercritical state, the surface tension vanishes and the gas-liquid phase interface blurs, and the breakup is replaced by turbulent mixing and diffusion process. Yang [3] and Bellan [4] presented comprehensive reviews on jet breakup, liquid evaporation and combustion, as well as provided important insights on the limitations of current basic theories and numerical methods

* Corresponding author, e-mail: lun_zhaomust@163.com

under supercritical conditions. As the ambient pressure increase from subcritical to supercritical conditions, the mixing mechanism and interface characteristics are less understood. Therefore, a systematic investigation on phase interface and mixing characteristics under trans/supercritical conditions is of great significance for fundamental research and practical applications.

With the development of experimental equipment, the injection mixing characteristics can be visualized at pressures close to or above the critical pressure of the injected fuel [5-10]. These experiments indicated that the classical breakup and atomization process can no longer be observed, but a dense fluid mixing process was very sensitive to small pressure and temperature disturbances, particularly at around its pseudo critical point. Oefelein *et al*. [11, 12] conducted experimental investigation on fuel injection using heptane or dodecane, these experiments showed that the fuel enters the chamber in the form of a compressed liquid, rather than the subcritical spray process, and the real fluid effects play a key role on supercritical conditions. Numerical approach is an alternative way to handle such complex and extreme condition. Zhu *et al*. [13, 14] investigated heptane droplets evaporation into nitrogen environment and reported the required pressure range for the droplet evaporation reached to its diffusion mixing state. Meng and Yang [15, 16] systematically studied the oxygen droplet evaporated into transcritical/supercritical hydrogen environment, with emphasis on evaporation characteristics and interaction of droplets. The results show that increasing the ambient pressure is beneficial to the evaporation of droplets and reduces the lifetime of the droplets, but the ambient temperature has little effect on droplet lifetime. Hsieh *et al.* [17] performed a numerical study on multi-component droplets near the critical state, and the results showed that the ambient pressure has significant influence on evaporation process, especially when the ambient pressure is close to the critical pressure, the conventional low pressure evaporation model will result in a higher evaporation rate.

In recent years, the molecular dynamics (MD) simulation had been widely used in nanoscale jet breakup [18-25] and supercritical heat transfer [26-36] due to the advantage of MD is that there is no need to make any assumptions about the process or physics. Therefore, MD solves all intermolecular interactions without considering any thermodynamic properties. Among of them, Moseler and Landman [19] are the typical to apply MD to the nanojet breakup of propane. The results indicated that the mechanism of nanojet rupture obtained by MD is significantly different from that of conventional continuous fluids. In droplet evaporation regime, Sumardiono and Fischer [26] investigated the influence of heat transfer on droplet evaporation. The density distribution of different evaporation periods was reported and gave out a method for counting the number of liquid atoms in liquid phase. Xie *et al*. [27] performed a simulation on condensation/evaporation and the dodecane velocity distribution at liquid-vapour phase equilibrium. The results showed that in the direction perpendicular to the surface, the evaporation coefficient increased as the molecular energy increases. Mo and Qiao [28] investigated the n-alkane fuels evaporated into nitrogen at different environmental conditions by MD simulation, and their emphasis was to study the transition conditions that the traditional two-phase evaporation transited into one phase diffusion-controlled mixing process. It can be found that the transition time is independent with the thickness of the liquid film, but it largely depends on the ambient conditions. Additionally, based on the P-T diagram, they proposed a threshold transition time of 0.35, which separates the subcritical from supercritical state.

In previous researches, most of the MD simulations on droplet evaporation were in subcritical conditions, and only few attentions were focused on the supercritical evaporation as well as the gas-liquid interface characteristics. In this study, the evaporation of n-heptane into nitrogen under different environment conditions by using MD simulation are investigated. Our concerns are focused on the mixing process between the droplet and ambient gas, furthermore,

liquid-gas interface characteristics based on the density profile under sub/supercritical conditions are defined to illustrate the mixing behavior. The conclusion obtained in MD simulation can be extended to microscopic regime and can help to provide a deep insight into microscopic mechanism of droplet evaporation process.

Molecular dynamics method and validation

Molecular dynamics method

To describe the microscopic dynamic characteristics of the system in MD simulation, the most important information input is the interatomic potential. In this study, n-heptane is chosen as the droplet evaporation, and the classical all-atom force fields OPLS-AA [37] is used due to its high accuracy for hydrocarbons fuels. The Lennard-Jones 12-6 potential for the non-bonded interaction is used and can be written:

$$U_{LJ} = 4\varepsilon\left[\left(\frac{\sigma}{r_{ij}}\right)^{12} - \left(\frac{\sigma}{r_{ij}}\right)^{6}\right] \tag{1}$$

where ε and σ are the potential energy and length parameters, respectively and r_{ij} is the distance between two atoms. The potential data can be shown in tab. 1.

Table 1. The parameters of OPLS-AA potential function

–	σ [nm]	ε [kcalmol^{-1}]	q [e]
C, RCH_3	0.350	0.066	–0.180
C, RCH_2	0.350	0.066	–0.120
H	0.250	0.030	0.060
N	0.325	0.170	0.000

In eq. (1), the arithmetic mixing rules are used for the interatomic potential in two different atoms:

$$\sigma_{ij} = \frac{1}{2}(\sigma_i + \sigma_j) \tag{2}$$

$$\varepsilon_{ij} = \sqrt{\varepsilon_i \varepsilon_j} \tag{3}$$

where i and j represent the different types of particles.

Simulation configuration

A rectangular simulation box of *gas-liquid-gas* model is employed to investigate the single droplet evaporation as shown in fig 1. A total of 1532 n-heptane molecules are fixed on the center, and the nitrogen molecules are placed on two sides. The dimensions of the simulation box in three directions x, y, and z are L_x, L_y, and L_z, respectively, and $L_x = 5L_y = 5L_z = 5L$, where $L = 7.4$ nm. The n-heptane liquid has an initial temperature of 363 K. According to the target pressure and temperature of the environment, nitrogen molecules are filled on both sides, which corresponding to subcritical, low supercritical, and high supercritical conditions. The simulation conditions are shown in tab. 2, where T_r and P_r are the corresponding temperature and corresponding pressure, respectively. In this simulation, liquid n-heptane and nitrogen were heated to 363 K and 800 K under NVT ensembles, respectively, after that the NVT ensembles were removed and the system was run in NVE ensembles. Initially, the velocity has a

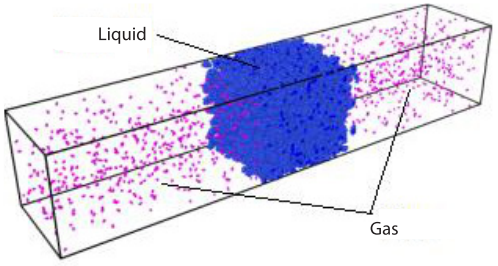

Figure 1. The simulation of *gas-liquid-gas* model

Maxwell-Boltzmann distribution, and Periodic boundary conditions are applied in *X*-, *Y*-, and *Z*-directions. In all simulations, the time step is 1 fs and the total simulation time is 2 ns. As the intermolecular distances increase, due to the rapid decay of the potential function, most molecular interactions are negligible. Hence, in this study, all the simulations used a cutoff distance of $r_c = 3.5\sigma$ to save calculation time. The standard velocity-verlet algorithm is applied to solve the equations of motion.

Table 2. The initial condition of subcritical and low/high supercritical environment

Case	N_{Hep}	T_{Hep}	N_{Nit}	T_{Nit}	T_r	P_r	ρ_{Hep}/ρ_{Nit}
Subcritical	1532	363	292	800	1.48	0.73	74.8
Low supercritical	1532	363	436	800	1.48	1.09	50.2
High supercritical	1532	363	1000	800	1.48	2.55	22.1

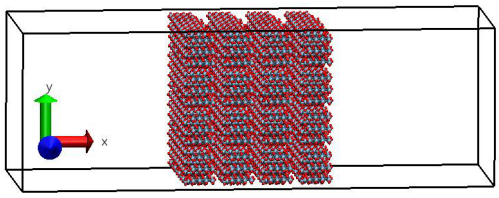

Figure 2. Simulation system of vacuum surroundings

Numerical verification of OPLS-AA force field

The gas/liquid surface model of Chapela and Saville [32] is applied to verify the OPLS-AA force field, which is shown in fig. 2. The system contains 896 n-heptane molecules, having a thickness of 12σ, which is placed on the center, while the left and right sides are vacuous. Initially, the velocity has a Maxwell-Boltzmann distribution, and periodic boundary conditions are applied in *X*-, *Y*-, and *Z*-directions. In all simulations, 2 fs of time step is taken and the total simulation time is 2 ns. Date is collected per 0.1 ns for statistical average calculation as the system reaching a stable state at 1 ns.

By counting on the microscopic particles, the macroscopic physical quantities such as density, temperature, and pressure can be obtained. Based on OPLS-AA force field, the gas-liquid interface characteristics at $T = 333$~493 K were shown in tab. 3. In the table, one can find that the liquid phase density distribution decreases with increasing the temperature, while the gas phase and interface thickness are exactly opposite. The results obtained in our simulation were agreed with Nijmeijer *et al*. [38], who performed a similar investigation on argon atoms evaporation.

Figure 3 shows the bulk density obtained by OPLS-AA force field and compare with experimental data [32]. The results show that the simulated density follows the trend well comparing to the experimental data. By close inspect, it can be found that the deviation increases with higher initial temperature of the droplet ($T > 433$ K). However, the simulated results agree well with the experiment at the temperature of below 433 K, with a relative error maintained within around 8%. Hence, the OPLS-AA force field is reliable in n-heptane calculation and can be used to investigate droplet evaporation in various pressure conditions.

Table 3. Numerical result of interfacial characterization under different temperature

T [K]	N	ρ_L [kgm^{-3}]	ρ_V [kgm^{-3}]	d [nm]
293	896	680.71	0.45	1.05
313	896	659.90	1.19	1.08
333	896	638.78	1.24	1.26
353	896	614.62	5.04	1.54
373	896	586.23	10.07	1.57
413	896	527.79	26.54	2.35
433	896	496.36	47.66	2.85
453	896	327.86	81.65	6.11
473	896	218.31	121.43	7.01
513	896	140.29	135.42	–
533	896	114.69	114.69	–

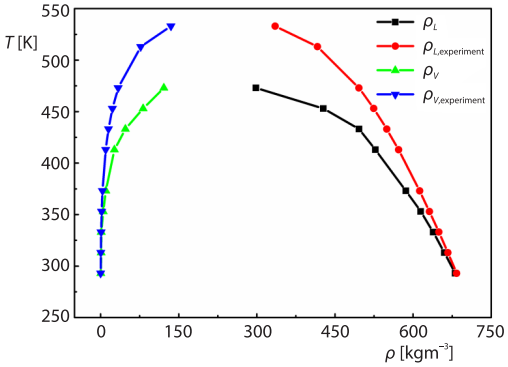

Figure 3. The density of the bulk phases

Results and discussions

The temperature distributions of the simulated box at different times for three cases are shown in fig. 4. It can be seen from the figure that the n-heptane molecules are struck due to the vigorous movement of the nitrogen molecules on both sides. The temperature on n-heptane

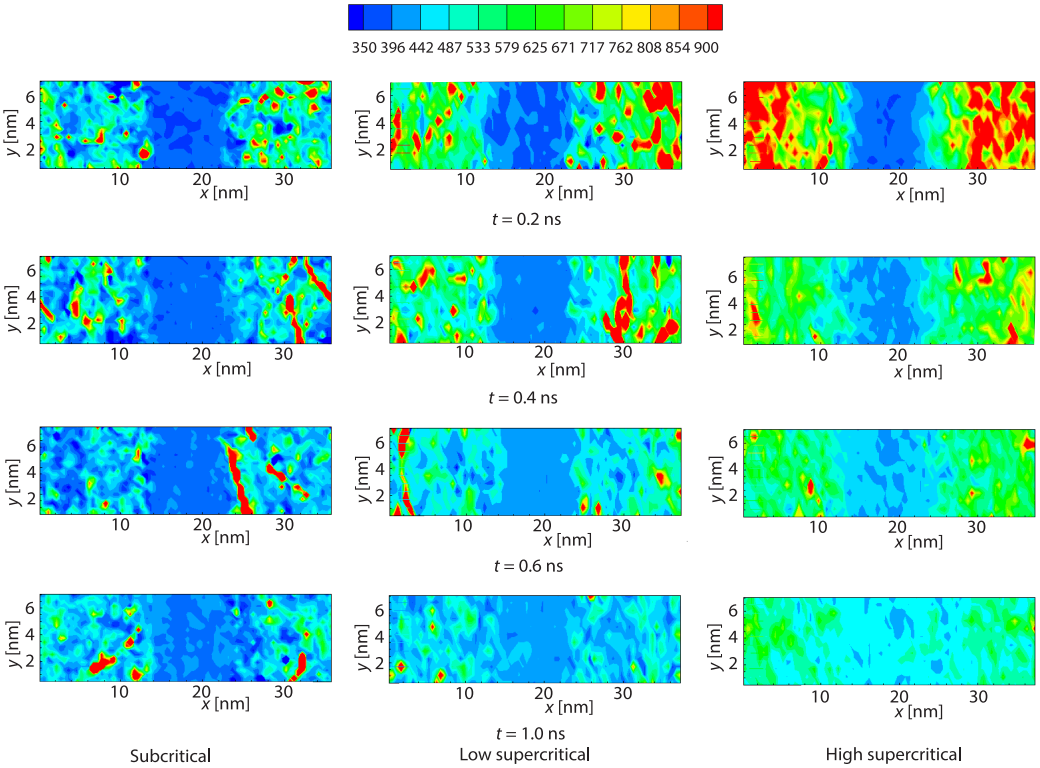

Figure 4. Comparison of temperature in the simulation box

is constantly increasing, while both nitrogen sides are exactly the opposite. This is because the nitrogen molecules transmit some of their energy to the n-heptane molecules through the collisions between molecules. By comparing different environment conditions at the same time, it is found that as the ambient pressure develops from subcritical to high supercritical, the temperature of n-heptane rises faster, while the temperature of nitrogen in subcritical conditions decreases rapidly. This is because for supercritical conditions, the amount of nitrogen molecules increases and contains larger energy due to the high pressure conditions. Therefore, the temperature of n-heptane increases faster under high supercritical conditions. Under high supercritical conditions, the n-heptane temperature is very close to the nitrogen temperature at t = 1.0 ns, and the molecular distribution is disordered. It is obvious that the high supercritical conditions facilitate heat exchange between the droplets and the ambient gas, promoting the droplet evaporation and mix with the surrounding fluid.

Figure 5 shows the comparison of n-heptane mass fractions at different times. It can be seen from the figure that as time progresses, n-heptane molecules continuously move to the nitrogen environment on both sides for three cases. At t = 1.0 ns, by comparing the three cases, we have two founding:

– Generally, it can be forming a larger mass fraction of n-heptane in both nitrogen districts under subcritical and low supercritical conditions.
– Under the high supercritical condition, the n-heptane spread a much wider region and the shape is confusing, with a decreasing of the mass fraction of n-heptane.

This can be due to the fact that there are large amount of initial nitrogen molecules existing in the nitrogen region under high supercritical condition. Although there are more n-heptane molecules moving into the nitrogen regions, the mass fraction is still lower.

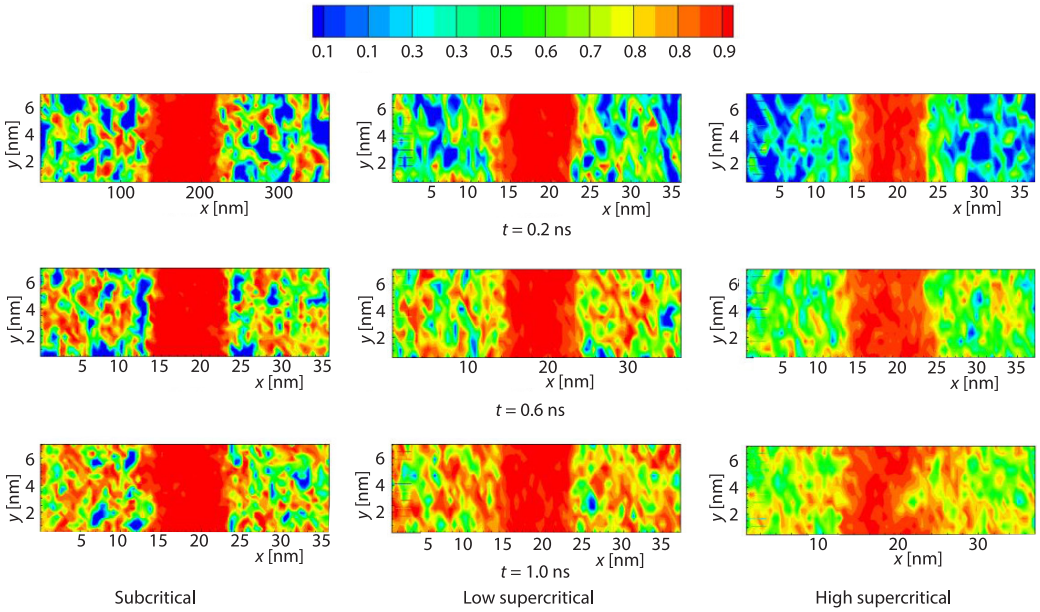

Figure 5. Comparison of n-heptane fraction distribution

To further understand the mixing characteristics of the *gas-liquid-gas* model under subcritical, low supercritical, and high supercritical conditions, the density distribution at t = 0.2 ns and 0.8 ns along the x-axis (half of the model) direction is shown in fig. 6. At t = 0.2

ns, since the initial density ratio (74.8) is highest under subcritical condition, the density distribution curve forms a large density gradient as transiting across the *gas-liquid* interface. As the ambient pressure continues to increase, the transition of n-heptane to nitrogen is relatively flat, and the interface is broadened, forming a thick mixed layer thickness. While $t = 0.8$ ns, the density of the n-heptane region of three cases decreased compared with $t = 0.2$ ns, and the high supercritical case decreased the fastest, indicating that many *n*-heptane molecules move to the nitrogen environment, so that the density of the nitrogen region is further increased, while the density gradient is further reduced. Hence the interface thickness is further broadened. These phenomena show that increasing the environmental pressure to a much high supercritical state will facilitate the mixing of the liquid n-heptane with the surrounding nitrogen molecules.

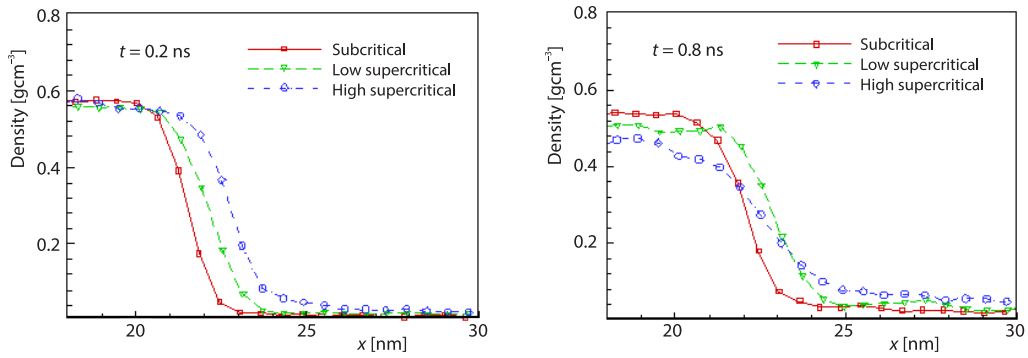

Figure 6. Comparison of density distribution

The temperature distribution of the simulated box along the *x*-axis direction for three cases is shown in fig. 7. Due to the heating effect of both high temperature nitrogen gas, energy transfer occurs through the collision of nitrogen molecules, n-heptane molecules gain more energy and the temperature of n-heptane is continuously increased, so the liquid temperature transit to the gas phase is relatively smooth, which forms a lower temperature gradient in the gas-liquid interface. In the early stage, due to the large temperature difference, the heat transfer is more intensive, and then gradually slows down. At $t = 0.8$ ns, the temperature difference is significantly reduced, and the temperature of the liquid phase is further increased, while the gas phase nitrogen is continuously reduced. The temperature of the liquid and gas becomes nearly equal until $t = 1.0$ ns. By comparison, it is found that at $t = 0.2$ ns and $t = 1.0$ ns, except for some extreme regions at both ends, except for some extreme regions at both ends, the temperature of the liquid and gas phase is much larger in the high supercritical case, followed by the low

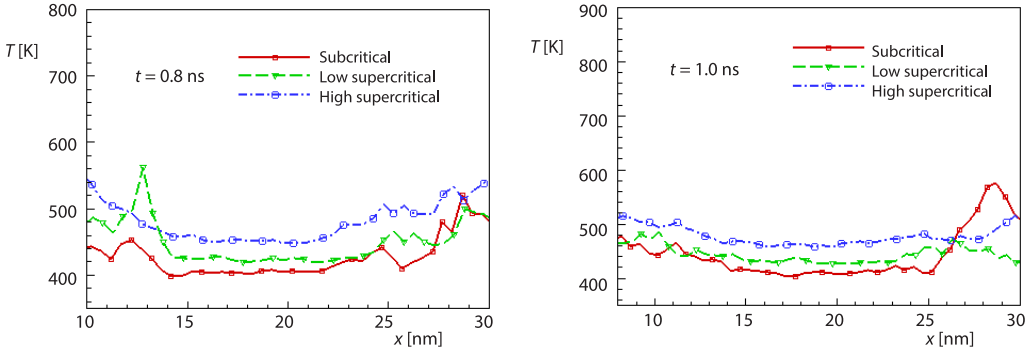

Figure 7. Comparison of temperature distribution

supercritical condition. These phenomena indicate that increasing the environmental pressure to a high supercritical condition helps to enhance the heat transfer characteristics between the gas and liquid phase, which is more advantageous for the mixing behavior. Figure 8 shows the mass fraction distribution of the simulated box along the *x*-direction. It can be seen from the figure that the high supercritical case has a lower mass fraction of n-heptane distribution in the gas regions, indicating that although there are more n-heptane molecules evaporating into the nitrogen region, the mass fraction of n-heptane is the lowest in the nitrogen gas district, which is consistent with the results observed in fig. 5.

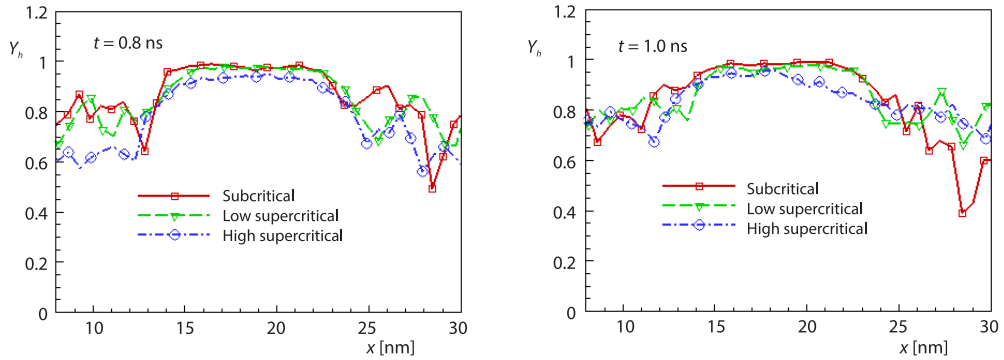

Figure 8. Comparison of n-heptane fraction distribution

In order to explore the influence of environmental pressure on the characteristics of gas-liquid interface, the whole simulated models are divided into 80 slices along the *x*-direction, and statistics are performed on the micro quantities to obtain the macroscopic density characteristics in each slice. Figure 9 shows the distribution of density in the *x*-direction. In this study, we define a gas-liquid *interface thickness*, which is the distance from the interface point with a density of $0.99\rho_{max}$ to the point where the value drops to $1.01\rho_{min}$ in the horizontal section along *x*-direction. According to this definition, the thickness of interface is also marked as shaded surface in fig. 9, and its values are summed in tab. 4. It is shown from the figure that the subcritical case has the smallest interface thickness, and the values become larger as the pressure increases. While the value of the high supercritical case is much higher than that of the subcritical case, and their value ratio is about 2.2. By carefully observing the evolution of the interface, we come to two findings. First of all, the interface thickness has a sharper decline in the low supercritical case as transiting across the interface region, second, the high supercritical case forms a smaller density distribution on the liquid side while shows a larger value in the interface area and gas side. Hence, as the environmental pressure increases to a much high supercritical state, a smaller initial density ratio (22.1) is formed, and the number of nitrogen molecules in the environment is larger, which promotes the heat exchange between the liquid and gas phase. Therefore, the thickness of gas-liquid interface is widened, ultimately resulting in a larger mixing layer thickness. For comparison, the results of Dahms and Oefelein [39] and Dahms *et al.* [40], who calculated the density profiles and interface thickness for both subcritical (T = 428 K, P = 3 MPa) and supercritical (T = 545 K, P = 6 MPa) conditions based on-linear Gradient Theory are shown in fig. 10. It is obvious that the as the pressure increase, the interface thickness becomes wider, which comes to the same conclusion with our investigation.

Table 4. Interface thickness based on density

Case	Subcritical	Lows supercritical	High supercritical
D [nm]	2.4	3.6	5.3

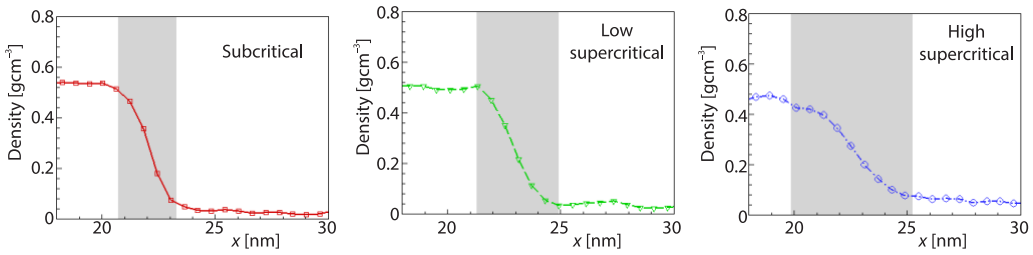

Figure 9. Mixing layer based on density distribution

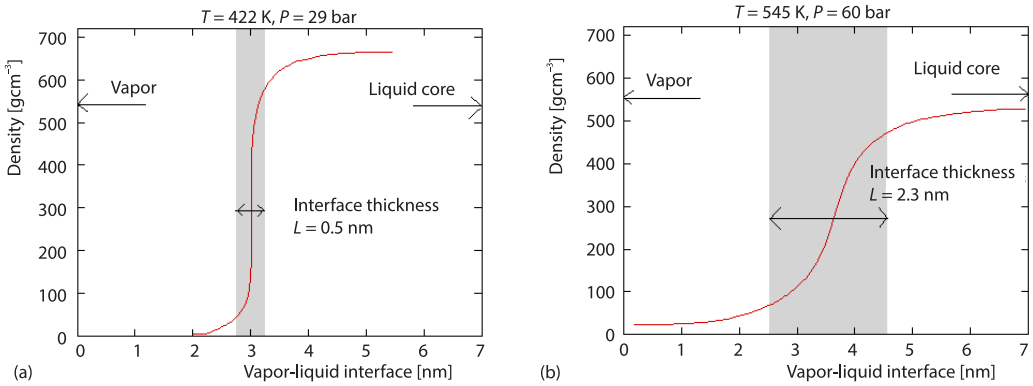

Figure 10. Vapor-liquid interface density profiles and thicknesses for the low-pressure (a) and high pressure (b) interface states, calculated using linear gradient theory [40]

Conclusions

In this study, we devote to examine the influence of environment pressure on the droplet evaporation characteristics by using the *gas-liquid-gas* model. The molecules of n-heptane liquid droplet evaporates into subcritical, low supercritical and high supercritical states are studied by MD. To validate the potential force field, the *gas-liquid-gas* models are used to simulate liquid n-heptane droplet evaporating into vacuum environment is simulated by OPLL-AA force field and compared with experiment.

As the pressure increase, the n-heptane droplet molecules tend to be evaporated into the nitrogen district and more nitrogen molecules begin to move into the n-heptane region due to the high collision frequency between n-heptane and nitrogen molecules, promoting energy exchange and the n-heptane molecules get more kinetic energy. Hence, as the ambient pressure develops from subcritical to high supercritical, the temperature of n-heptane raise faster, while the temperature of nitrogen in subcritical conditions decreases rapidly. For the same reason, the mass fraction of n-heptane decrease in the liquid region and spread a much wider region and the shape is confusing. While in the nitrogen district, the mass fraction decrease with increasing of the ambient pressure due to a large amount of initial nitrogen molecules existing in the nitrogen region under high supercritical condition. Based on the density profile, a *gas-liquid-gas* interface thickness is defined and the interface thickness is widened as the ambient pressure increase, suggesting that increasing the ambient pressure, the interface tension gradually decrease, and the gas-liquid interface broaden, resulting in the conventional subcritical evaporation transition turbulent mixing process. However, to *what conditions* and *what time* the transition process will take place is less well understood. Hence, in the further study, we will perform a fundamental research on these two aspects.

Acknowledgments

This work is supported by National Natural Science Foundation of China (Grant No. 52066004 and No. 51576029). Guizhou Science and Technology Plan Project (Grant No. 20201Y237). Guizhou University introduces talent research (Grant No. 201819).

References

[1] Ahn, Y., *et al*., Review of Supercritical CO_2 Power Cycle Technology and Current Status of Research and Development, *Nuclear Engineering & Technology*, *47* (2015), 6, pp. 647-661
[2] Knez, Ž., *et al.*, Industrial Applications of Supercritical Fluids: A Review, *Energy*, *77* (2014), Dec., pp. 235-243
[3] Yang, V., Modelling of Supercritical Vaporization, Mixing, and Combustion Processes in Liquid-Fueled Propulsion Systems, *Proceedings of the Combustion Institute*, *28* (2000), 1, pp. 925-942
[4] Bellan, L., Supercritical (and Subcritical) Fluid Behavior and Modelling: Drops, Streams, Shear and Mixing Layers, Jets and Sprays, *Progress in Energy & Combustion Science*, *26* (2000), 4-6, pp. 329-366
[5] Oschwald, M., Schik, A., Supercritical Nitrogen Free Jet Investigated by Spontaneous Raman Scattering, *Experiments in Fluids*, *27* (1999), Nov., pp. 497-506
[6] Chehroudi, B., *et al*., Cryogenic Shear Layers: Experiments and Phenomenological Modelling of the Initial Growth Rate under Subcritical and Supercritical Conditions, *International Journal of Heat & Fluid-Flow*, *23* (2002), 5, pp. 554-563
[7] Chehroudi, B., *et al*., Visual Characteristics and Initial Growth Rates of Round Cryogenic Jets at Subcritical and Supercritical Pressures, *Physics of Fluids*, *14* (2002), 2, pp. 850-861
[8] Branam, R., Mayer, W., Characterization of Cryogenic Injection at Supercritical Pressure, *Journal of Propulsion & Power*, *19* (2003), 3, pp. 342-355
[9] Mayer, W., *et al*., Raman Measurements of Cryogenic Injection at Supercritical Pressure, *Heat & Mass Transfer*, *39* (2003), July, pp. 709-719
[10] Segal, C., Polikhov, S. A., Subcritical to Supercritical Mixing, *Physics of Fluids*, *20* (2008), 5, 052101
[11] Oefelin, J., Analysis of Transcritical Spray Phenomena in Turbulent Mixing Layers, *Proceedings*, 34th Aerospace Sciences Meeting and Exhibit, Reno, Nev., USA, 1996
[12] Oefelein, J. C., Yang, V., Modelling High-Pressure Mixing and Combustion Processes in Liquid Rocket Engines, *Journal of Propulsion & Power*, *14* (1998), 5, pp. 843-857
[13] Zhu , G. S., S. K. Aggarwal, S. K, Transient Supercritical Droplet Evaporation with Emphasis on the Effects of Equation of State, *International Journal of Heat & Mass Transfer*, *43* (2000), 7, pp. 1157-1171
[14] Zhu, G. S., *et al*., Gas-Phase Unsteadiness and Its Influence on Droplet Vaporization in sub- and super-Critical Environments, *International Journal of Heat & Mass Transfer*, *44* (2001), 16, pp. 3081-3093
[15] Meng, H., Yang, A., Clustering Effects on Liquid Oxygen (LOX) Droplet Vaporization in Hydrogen Environments at Subcritical and Supercritical Pressures, *International Journal of Hydrogen Energy*, *37* (2012), 16, pp. 11815-11823
[16] Meng, H., Yang, V., Vaporization of Two Liquid Oxygen (LOX) Droplets in Tandem in Convective Hydrogen Streams at Supercritical Pressures, *International Journal of Heat & Mass Transfer*, *68* (2014), Jan., pp. 500-508
[17] Hsieh, K. C., *et al*., Droplet Vaporization in High-Pressure Environments I: Near Critical Condition, *Combustion Science & Technology*, *76* (1991), 1-3, pp. 111-132
[18] Branam, R. D., Molecular Dynamics Simulation of Supercritical Fluids, Ph. D. thesis, The Pennsylvania State University, State College, Penn., USA, 2005
[19] Moseler, M., Landman, U., Formation, Stability, and Breakup of Nanojets, *Science*, *289* (2000), 5582, pp. 1165-1169
[20] Micci, M. M., *et al*., Molecular Dynamics Simulations of Atomization and Spray Phenomena, *Atomization & Sprays*, *11* (2001), 4, pp. 351-363
[21] Shin, H. H., Yoon, W. S., Non-Equilibrium Molecular Dynamics Simulation of Nanojet Injection with Adaptive-Spatial Decomposition Parallel Algorithm, *Journal of Nanoscience & Nanotechnology*, *8* (2008), 3661
[22] Shin, H. H., *et al*., Non-Equilibrium Molecular Dynamics of Nanojet Injection in a High Pressure Environment, *Micro-fluidics & Nanofluidics*, *5* (2008), 4, pp. 561-570
[23] Fang, T. H., *et al*., Effects of Temperature and Aperture Size on Nanojet Ejection Process by Molecular Dynamics Simulation, *Microelectronics Journal*, *35* (2004), 9, pp. 687-691

[24] Choi, Y. S, *et al*., Molecular Dynamics of Unstable Motions and Capillary Instability in Liquid Nanojets, *Phys. Rev. E Stat. Non-Lin. Soft. Matter. Phys*, *73* (2006), 016309
[25] Wei, W., *et al*., Non-Equilibrium Molecular Dynamics Modelling of a Fuel Nanojet in Sub/Supercritical Environments: Chamber Pressure Effects on Characteristics of the Gas-Liquid Interface, *Nanoscale & Microscale Thermophysical Engineering*, *22* (2017), 1, pp. 52-66
[26] Sumardiono, S., Fischer, J., Molecular Simulations of Droplet Evaporation by Heat Transfer, *Micro-Fluidics & Nanofluidics*, *3* (2006), Sept., pp. 127-140
[27] Xie, J. F., *et al*., Molecular Dynamics Study of Condensation/Evaporation and Velocity Distribution of N-Dodecane at Liquid-Vapour Phase Equilibria, *Journal of Thermal Science & Technology*, *7* (2012), 1, pp. 288-300
[28] Mo, G., Qiao, L., A Molecular Dynamics Investigation of n-Alkanes Vaporizing into Nitrogen: Transition from Subcritical to Supercritical, *Combustion & Flame*, *176* (2017), Feb., pp. 60-71
[29] Landry, E. S., *et al*., Droplet Evaporation: A Molecular Dynamics Investigation, *Journal of Applied Physics*, *102* (2007), 12, 124301
[30] Walther, J. H., Koumoutsakos, P., Molecular Dynamics Simulation of Nanodroplet Evaporation, *Journal of Heat Transfer*, *123* (2001), 4, pp. 741-748
[31] Kaltz, T. L., *et al*., Supercritical Vaporization of Liquid Oxygen Droplets Using Molecular Dynamics, *Combustion Science & Technology*, *136* (1998), 1-6, pp. 279-301
[32] Chapela, G. A., *et al*., Computer Simulation of the Gas/Liquid Surface, *Faraday Discussions of the Chemical Society*, *59* (1975), pp. 22-28
[33] Chapela, G. A., *et al*., Computer Simulation of a Gas-Liquid Surface – Part 1: *Journal of the Chemical Society Faraday Transactions*, *73* (1977), 7, pp. 1133-1144
[34] Benarous, A., Liazid, A., The H_2O_2 Supercritical Combustion Modelling Using a CFD Code, *Thermal Science*, *13* (2009), 3, pp. 139-152
[35] Sarkar, J., Improving Thermal Performance of Micro-Channel Electronic Heat Sink Using Supercritical CO_2 as Coolant, *Thermal Science*, *23* (2019), 1, pp. 243-253
[36] Yue, H. Y., Liu, Z. G., Viscosity Prediction of Refrigerants under Subcritical/Supercritical Conditions, *Thermal Science*, *19* (2015), 4, pp. 1293-1296
[37] Jorgensen, W. L., *et al*., Development and Testing of the OPLS all-Atom Force Field on Conformational Energetics and Properties of Organic Liquids, *Journal of the American Chemical Society*, *118* (2017), 45, pp. 11225-11236
[38] Nijmeijer, M. J. P., *et al*., A Molecular Dynamics Simulation of the Lennard-Jones Liquid-Vapor Interface, *Journal of Chemical Physics*, *89* (1988), 6, pp. 3789-3792
[39] Dahms, R. N., Oefelein, J. C., Non-Equilibrium Gas-Liquid Interface Dynamics in High-Pressure Liquid Injection Systems, *Proceedings of the Combustion Institute*, *35* (2013), 2, pp. 1587-1594
[40] Dahms, R. N., *et al*., Understanding High-Pressure Gas-Liquid Interface Phenomena in Diesel Engines, *Proceedings of the Combustion Institute*, *34* (2013), 1, pp. 1667-1675

Paper submitted: February 1, 2021
Paper revised: September 18, 2021
Paper accepted: September 30, 2021